

# A Straightforward $hp$ -Adaptivity Strategy for Shock-Capturing with High-Order Discontinuous Galerkin Methods

Hongqiang Lu\* and Qiang Sun

College of Aerospace Engineering, Nanjing University of Aeronautics and Astronautics,  
Nanjing 210016, China

Received 15 October 2012; Accepted (in revised version) 17 October 2013

Available online 13 December 2013

---

**Abstract.** In this paper, high-order Discontinuous Galerkin (DG) method is used to solve the two-dimensional Euler equations. A shock-capturing method based on the artificial viscosity technique is employed to handle physical discontinuities. Numerical tests show that the shocks can be captured within one element even on very coarse grids. The thickness of the shocks is dominated by the local mesh size and the local order of the basis functions. In order to obtain better shock resolution, a straightforward  $hp$ -adaptivity strategy is introduced, which is based on the high-order contribution calculated using hierarchical basis. Numerical results indicate that the  $hp$ -adaptivity method is easy to implement and better shock resolution can be obtained with smaller local mesh size and higher local order.

**AMS subject classifications:** 35L67, 65M60

**Key words:**  $hp$ -adaptivity, shock capturing, discontinuous Galerkin.

---

## 1 Introduction

Discontinuous Galerkin (DG) methods [1–10] have recently become more and more popular for the solution of the Euler and Navier-Stokes equations of gas dynamics [1, 4, 5, 8, 10]. DG methods combine two important features which commonly characterize the finite element and finite volume methods. Firstly, high-order solutions can be obtained via using high-order polynomial approximation inside elements. Furthermore, upwinding can be easily implemented through using appropriate numerical fluxes over element interfaces. These two features make DG methods suitable for convection-dominated problems and highly accurate solutions can be obtained on relatively coarse grids if high-order scheme is used.

---

\*Corresponding author.

Email: hongqiang.lu@nuaa.edu.cn (H. Lu)

However, for the cases involving strong discontinuities (for example, the shocks in the transonic flows and supersonic flows), the unlimited high-order solution oscillates near the discontinuities. There are many methods that can be used to eliminate the numerical oscillations. The most straightforward one is to reduce the order of the polynomial near the shocks. However, the accuracy of the scheme can be seriously degraded. Hence, the mesh-refinement has to be used to provide a satisfactory solution. The weighted essentially non-oscillatory (WENO) schemes can also be used since they provide stable discretization near discontinuities and still maintain high-order accuracy. The main drawback is that they become to be highly consuming when the degree of the approximating polynomial is increased. There are also some other methods based on reconstructing the oscillatory solutions computed using a high order method. But it is still an issue to extend these methods to multiple dimensions. Recently, an artificial viscosity method (sub-cell shock-capturing method) was introduced to capture the shocks when high-order DG is used [10]. In this method, the accuracy of the solution in the neighborhood of the shock becomes  $\mathcal{O}(h/p)$  and the shock profile can be resolved in one element when high order is used.

In this paper, the high-order DG methods combined with the sub-cell shock-capturing technique are used to simulate compressible flows with shocks. The diffusion term introduced by the artificial viscosity technique is discretized using LDG [2] scheme as shown in [10]. Newton method [4] is employed to solve the nonlinear discrete systems. For each nonlinear iteration, the resultant sparse linear system is solved using a block-Gauss Seidel method. Since Newton method is relatively sensitive to the initial guess, a hierarchical solution procedure is suggested in this paper.

Numerical results indicate that the shocks can be well resolved inside one element when the above artificial viscosity technique is used. However, the shock thickness is dominated by the local order and the local mesh size. In order to reach the required shock thickness, an  $hp$ -adaptivity method is introduced in this work. Firstly, a smoothness sensor based on the high-order contribution is used to detect the position of the shocks. Secondly, the local order of the basis is enhanced to improve the resolution. If the solution near the shocks is still not accurate enough when the local order reaches 4, the local mesh will be refined. Numerical results show that the straightforward  $hp$ -adaptivity strategy can produce reasonable mesh structure and order distribution which can provide accurate shock resolution at relatively low expense.

## 2 Governing equations

The two-dimensional Euler equations in conservative form can be written as

$$\frac{\partial \mathbf{U}}{\partial t} + \nabla \cdot \mathbf{F}(\mathbf{U}) = 0, \quad (2.1)$$

where the conservative variables  $\mathbf{U}$  and the components  $\mathbf{f}(\mathbf{U})$  and  $\mathbf{g}(\mathbf{U})$  of  $\mathbf{F}(\mathbf{U})$  are given by

$$\mathbf{U} = \begin{bmatrix} \rho \\ \rho v_1 \\ \rho v_2 \\ \rho e \end{bmatrix}, \quad \mathbf{f}(\mathbf{U}) = \begin{bmatrix} \rho v_1 \\ \rho v_1^2 + P \\ \rho v_1 v_2 \\ \rho h v_1 \end{bmatrix}, \quad \mathbf{g}(\mathbf{U}) = \begin{bmatrix} \rho v_2 \\ \rho v_1 v_2 \\ \rho v_2^2 + P \\ \rho h v_2 \end{bmatrix}, \quad (2.2)$$

where  $\rho$ ,  $P$  and  $e$  denote the density, pressure and the total internal energy per unit mass respectively.  $v_1$  and  $v_2$  are the velocity components. The total enthalpy per unit mass  $h$  is defined as  $h = e + p/\rho$ . For perfect gas,  $P = (\gamma - 1)\rho(e - (v_1^2 + v_2^2)/2)$ , where  $\gamma$  is the ratio of the specific heats.

### 3 DG discretization

The weak formulation of Eq. (2.1) can be obtained by multiplying a test function  $W$ , integrating over the domain  $\Omega$  and performing an integration by parts

$$\int_{\Omega} W \frac{\partial \mathbf{U}}{\partial t} d\Omega + \int_{\partial\Omega} W \mathbf{F}(\mathbf{U}) \cdot \mathbf{n} d\delta - \int_{\Omega} \nabla W \cdot \mathbf{F}(\mathbf{U}) d\Omega = 0, \quad \forall W, \quad (3.1)$$

where  $\partial\Omega$  is the boundary of  $\Omega$ .

By subdividing the domain into a collection of non-overlapping triangle elements, the semi-discrete equations for  $\Omega_e$  can be written as

$$\frac{\partial}{\partial t} \int_{\Omega_e} W_h \mathbf{U}_h d\Omega + \int_{\partial\Omega_e} W_h \mathbf{F}(\mathbf{U}_h) \cdot \mathbf{n} d\delta - \int_{\Omega_e} \nabla W_h \cdot \mathbf{F}(\mathbf{U}_h) d\Omega = 0, \quad \forall W_h, \quad (3.2)$$

where  $\mathbf{U}_h$  and  $W_h$  are the finite element approximations to  $\mathbf{U}$  and  $W$

$$\mathbf{U}_h(X, t) = \sum_{m=1}^{N(p)} u_m(t) \phi_m(X), \quad (3.3a)$$

$$W_h(X, t) = \sum_{m=1}^{N(p)} w_m(t) \phi_m(X), \quad (3.3b)$$

where  $\phi_m(X)$  are the basis functions of degree  $p$ . Here the hierarchical basis functions are used [6,7]. Since  $W_h$  are a linear combination of  $N(p)$  shape functions  $\phi_m(X)$ , Eq. (3.2) is equivalent to the following system

$$\frac{\partial}{\partial t} \int_{\Omega_e} \phi_i \mathbf{U}_h d\Omega + \int_{\partial\Omega_e} \phi_i \mathbf{F}(\mathbf{U}_h) \cdot \mathbf{n} d\delta - \int_{\Omega_e} \nabla \phi_i \cdot \mathbf{F}(\mathbf{U}_h) d\Omega = 0, \quad 1 \leq i \leq N(p). \quad (3.4)$$

Since DG allows discontinuities over element interfaces, flux terms are not unique at element interfaces. The flux function  $\mathbf{F}(\mathbf{U}_h) \cdot \mathbf{n}$  in Eq. (3.4) is replaced by a numerical

flux function  $\mathbf{H}(\mathbf{U}_h^-, \mathbf{U}_h^+, \mathbf{n})$ , which is calculated using the internal interface state  $\mathbf{U}_h^-$ , the neighboring element interface state  $\mathbf{U}_h^+$  and the direction normal  $\mathbf{n}$ . In this paper, the LLF flux is used [4].

In order to eliminate the numerical oscillations near shocks, the sub-cell shock capturing method [10] is used, for which an auxiliary diffusion term is added to the original Euler equations (2.1)

$$\frac{\partial \mathbf{U}}{\partial t} + \nabla \cdot \mathbf{F}(\mathbf{U}) = \nabla \cdot (\varepsilon \nabla \mathbf{U}), \quad (3.5)$$

where  $\varepsilon$  is the artificial viscosity, which is defined by

$$\varepsilon_e = \begin{cases} 0, & \text{if } s_e \leq s_0 - k, \\ \frac{\varepsilon_0}{2} \left( 1 + \sin \left( \frac{\pi(s_e - s_0)}{2k} \right) \right), & \text{if } s_0 - k \leq s_e \leq s_0 + k, \\ \varepsilon_0, & \text{if } s_e \geq s_0 + k. \end{cases} \quad (3.6)$$

Here  $\varepsilon_0 \approx h/p$ ,  $s_0 \approx 1/p^4$  and  $k$  is chosen sufficiently large to obtain a sharp but smooth shock profile.  $s_e = \log(S_e)$ , where  $S_e$  is a smoothness indicator which evaluates the local highest order contribution [6] of  $\mathbf{U}$

$$S_e = \frac{(\mathbf{U} - \mathbf{U}^{p-1})_e}{(\mathbf{U}, \mathbf{U})_e}. \quad (3.7)$$

Here  $(\cdot, \cdot)_e$  is the standard inner product in  $L_2(\Omega_e)$  and

$$\mathbf{U}^{p-1} = \sum_{i=1}^{N(p-1)} u_i \phi_i. \quad (3.8)$$

LDG [2] is used to discretize the diffusion term by splitting Eq. (3.5) into

$$\mathbf{Q} - \varepsilon \nabla \mathbf{U} = 0, \quad (3.9)$$

and

$$\frac{\partial \mathbf{U}}{\partial t} + \nabla \cdot \mathbf{F}(\mathbf{U}) - \nabla \cdot \mathbf{Q} = 0, \quad (3.10)$$

where  $\mathbf{Q}$  is an auxiliary variable.

The weak formulation of Eq. (3.9) is

$$\int_{\Omega_e} \phi_i \mathbf{Q}_h d\Omega + \int_{\partial\Omega_e} \phi_i \varepsilon \mathbf{U}_h \mathbf{n} d\delta + \int_{\Omega_e} \nabla \phi_i \varepsilon \mathbf{U}_h d\Omega = 0, \quad (3.11)$$

where the  $\mathbf{U}_h \mathbf{n}$  is replaced by a numerical flux

$$\mathbf{H}(\mathbf{U}^-, \mathbf{U}^+, \mathbf{n}) = \frac{1}{2} (\mathbf{U}^- + \mathbf{U}^+) \mathbf{n}. \quad (3.12)$$

Recall Eq. (3.4), the weak form of Eq. (3.10) can be written as

$$\begin{aligned} \frac{\partial}{\partial t} \int_{\Omega_e} \phi_i \mathbf{U}_h d\Omega + \int_{\partial\Omega_e} \phi_i \mathbf{H}(\mathbf{U}^-, \mathbf{U}^+, \mathbf{n}) d\delta - \int_{\Omega_e} \nabla \phi_i \cdot \mathbf{F}(\mathbf{U}_h) d\Omega \\ - \int_{\partial\Omega_e} \phi_i \mathbf{Q}_h \cdot \mathbf{n} d\delta + \int_{\Omega_e} \nabla \phi_i \cdot \mathbf{Q}_h d\Omega = 0, \end{aligned} \tag{3.13}$$

where  $\mathbf{Q}_h \cdot \mathbf{n}$  is replaced by a numerical flux

$$\mathbf{H}_Q(\mathbf{Q}^-, \mathbf{Q}^+, \mathbf{n}) = \frac{1}{2}(\mathbf{Q}^- + \mathbf{Q}^+) \cdot \mathbf{n}. \tag{3.14}$$

### 4 Relaxation

The Newton method can be used to solve the final nonlinear system in Eq. (3.13)

$$\mathbf{U}^{n+1} \leftarrow \mathbf{U}^n + C\Delta\mathbf{U}^n, \tag{4.1}$$

where  $C$  is the under-relaxation factor and  $\Delta\mathbf{U}^n$  is obtained by solving the following linear system

$$\mathbf{A}(\mathbf{U}^n)\Delta\mathbf{U}^n = \mathbf{R}(\mathbf{U}^n), \quad \mathbf{A}(\mathbf{U}^n) = \frac{-\partial\mathbf{R}(\mathbf{U}^n)}{\partial\mathbf{U}^n}. \tag{4.2}$$

Note that  $\mathbf{A}(\mathbf{U}^n)$  is a sparse block matrix (see Fig. 1) and the block size would be different when  $hp$ -adaptivity is employed. Only the non-zero blocks need to be stored and the linear system (4.2) arising for each Newton iteration is solved using Block Gauss-Seidel method.

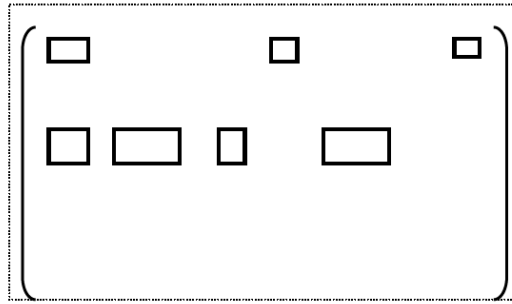


Figure 1: The structure of  $-\partial\mathbf{R}(\mathbf{U}^n)/\partial\mathbf{U}^n$ .

In order to improve the conditioning of the linear system (4.2), a pseudo-time derivative can be added to original discrete system [5]

$$\mathbf{R}(\mathbf{U}^n) = \mathbf{R}(\mathbf{U}^n) - \left( \frac{\mathbf{U}^n - \mathbf{U}^{n-1}}{\Delta T^n}, W \right). \tag{4.3}$$

It can be easily observed from Eqs. (4.2) and (4.3) that the new  $\mathbf{A}(\mathbf{U}^n)$  will become diagonally dominant with small  $\Delta T^n$ , which makes the Block Gauss-Seidel method easier to converge.

## 5 *hp*-adaptivity strategy

It is reported in [10] that the shocks can be captured inside one element when high order scheme is used and  $p = 4$  is suggested for computational stability and accuracy reason of shock-capturing approach. In this paper, a *hp*-adaptivity strategy is developed to capture shocks with relatively low computational expense. For the *p*-adaptivity, the highest order  $p_{\max}$  over the entire domain is limited to 4. For the *h*-adaptivity, the minimum mesh size  $h_{\min}$  is pre-defined. The *hp*-adaptivity strategy will search for a reasonable *hp*-distribution under the limit of  $p_{\max}$  and  $h_{\min}$ .

### 5.1 Adaptivity sensor

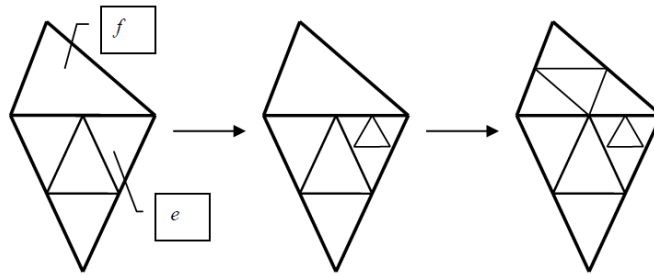
In this paper, the entire solution procedure will start from  $p = 0$  on a very coarse initial grid. Then the order  $p$  will be increased and the mesh will be refined in the region where the solution is not smooth enough (normally near the shocks). So an adaptivity sensor (or shock sensor) is needed to determine the region to be refined.

As we can see in Eq. (3.6),  $\varepsilon$  becomes nonzero in the region where the solution is not smooth enough. Then  $\varepsilon_e$  or  $S_e$  can be used as an adaptivity sensor. Here a tolerance  $\varepsilon_{Tol}$  or  $S_{e,Tol}$  is given. Once  $\varepsilon_e \geq \varepsilon_{Tol}$  or  $S_e \geq S_{e,Tol}$ , the local order is to be enhanced if  $p < 4$ .

### 5.2 Full solution procedure

The Newton method often requires a relatively good initial guess to ensure the convergence, or a very small under-relaxation factor  $C$  has to be used. To ensure the stability of convergence of the Newton method, we use the following global solution procedure:

1. Start with  $p=0$  and set the initial guess to be the far-field flow. Obtain  $p=0$  solution using Newton-Block Gauss-Seidel method.
2. Interpolate the  $p=0$  solution to  $p=1$  space and obtain a  $p=1$  solution using Newton-Block Gauss-Seidel method.
3. Evaluate  $\varepsilon_e$  or  $S_e$ . When  $\varepsilon_e \geq \varepsilon_{Tol}$  or  $S_e \geq S_{e,Tol}$ , increase  $p_e$  if  $p_e < 4$  or refine the element  $e$  if  $p_e = 4$ . Reduce the order from  $p_e$  to  $p_e - 1$  if the local solution is smooth enough (for example,  $\varepsilon_e \geq \varepsilon_{Tol,1}$  or  $S_e \geq S_{e,Tol,1}$ , where  $\varepsilon_{Tol,1}$  or  $S_{e,Tol,1}$  are very small).
4. Keep repeating the above *hp*-adaptivity step until the minimum mesh size reaches a given tolerance  $h_{\min}$ .
5. Stop the entire iteration when the  $R^2$ -norm of the residual is reduced to  $\mathcal{O}(-10)$ .

Figure 2: The smoothing strategy for  $h$ -adaptivity.

To ensure the stability of the Newton-Block Gauss-Seidel relaxation, the pseudo-time derivative in Eq. (4.3) is used together with a relatively small under-relaxation factor.

In order to avoid the large gradient of mesh size between neighboring elements, a smoothing strategy for  $h$ -adaptivity is employed. For example, if the element  $e$  in Fig. 2 is refined according to the local  $\varepsilon_e$  or  $S_e$ , the neighboring element  $f$  will also be refined to avoid extreme difference in local mesh size.

## 6 Numerical results

The transonic ( $Ma = 0.8$ ,  $\alpha = 1.5^\circ$ ) flow around the NACA0012 airfoil is simulated here. The initial mesh contains 796 elements, 431 grid points, and only 48 grid points on the solid boundary (see Fig. 3).

Fig. 4 demonstrates the Mach contours obtained with uniform orders ( $p = 1, 2, 3, 4$ ) over the entire domain on the initial grid. It can be clearly observed that the resolution of the shocks can be significantly improved when the order is increased, which implies that higher order scheme should be used near the shocks for better resolution. Fig. 5 indicates

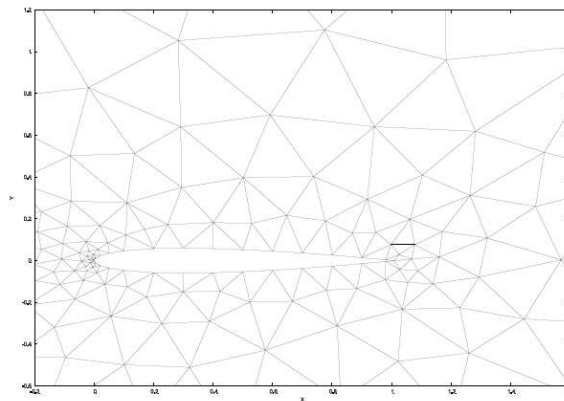


Figure 3: The initial grid.

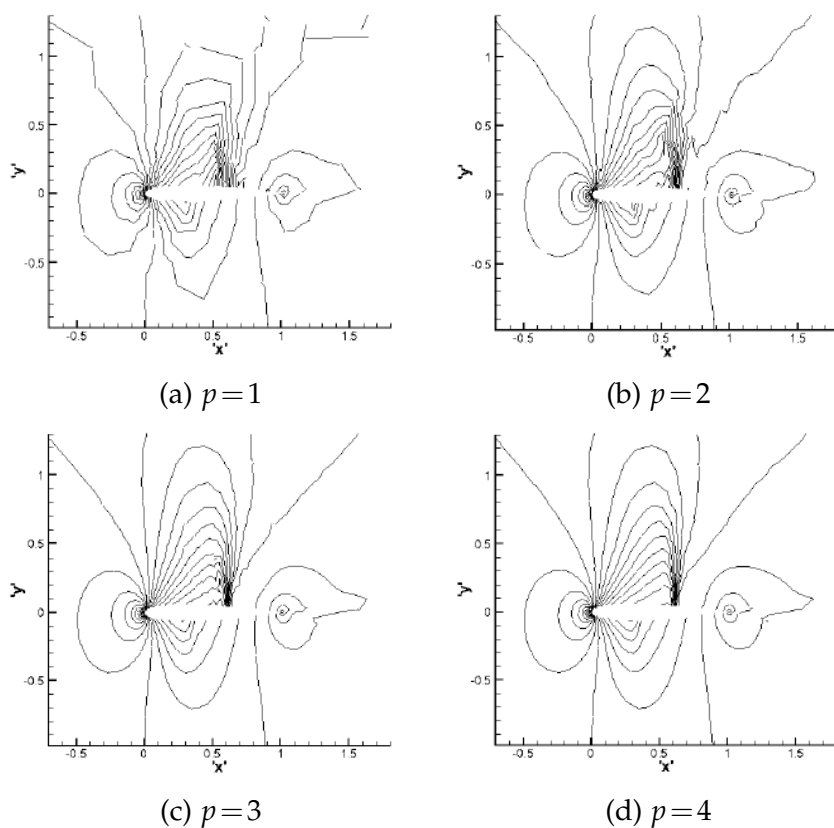


Figure 4: The Mach contours with increasing uniform orders ( $p=1\sim 4$ ) on the initial grid.

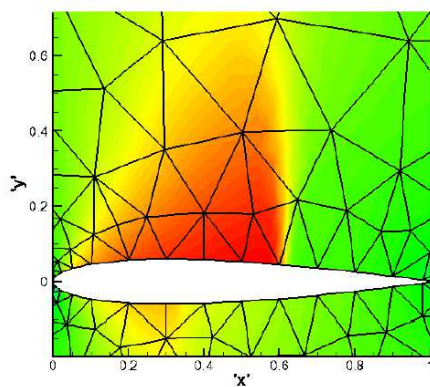


Figure 5: The Mach contours and the local mesh when  $p=4$ .

that the shocks can be captured inside one element when high-order scheme is used [10], which suggests smaller mesh size for thinner shock resolution.

To improve the accuracy of the shocks and reduce the computational expense, the local  $hp$ -adaptivity method introduced above is used to calculate the same transonic case.

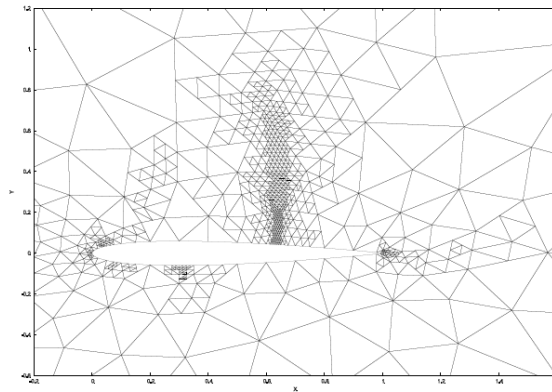


Figure 6: The final mesh distribution.

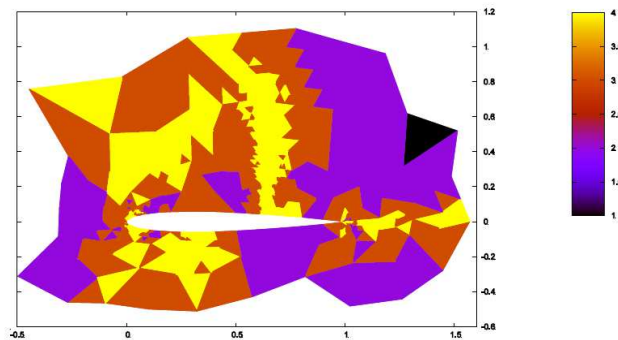
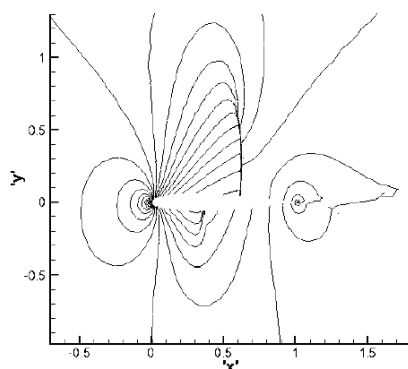


Figure 7: Order distribution.

Figs. 6 and 7 show the final mesh distribution and the order distribution, where only the local mesh and the local order near the shocks have been refined and increased. Fig. 8 depicts the obtained Mach contours, where the shock captured on the upper surface is much thinner since the local mesh size is much smaller as compared to the uniform  $p = 4$  case in Fig. 5.

## 7 Conclusions

An artificial viscosity technique is used to handle the physical discontinuities for the DG solution of the Euler Equations. LDG is employed to discretize the diffusion term introduced by the artificial viscosity technique. In order to obtain better resolution of the shocks, a straightforward  $hp$ -adaptivity strategy based on the high-order contribution is introduced in this work. Numerical results show that the  $hp$ -adaptivity method can result in reasonable mesh distribution and order distribution, which makes capturing shocks more accurately at lower expense.

Figure 8:  $Ma$  contours.

## Acknowledgments

Thanks for the foundation of the National Natural Science Foundation of China (11272152) and the Aeronautical Science Foundation of China (20101552018).

## References

- [1] F. BASSI AND S. REBAY, *High-order accurate discontinuous finite element solution of the 2d Euler equations*, J. Comput. Phys., 138 (1997), pp. 251–285.
- [2] B. COCKBURN AND C. W. SHU, *The local discontinuous Galerkin method for time-dependent convection-diffusion systems*, SIAM J. Numer. Anal., 35 (1998), pp. 2440–2463.
- [3] B. COCKBURN, G. E. KARNIADAKIS AND C. W. SHU, *Discontinuous Galerkin Methods: Theory, Computation and Applications*, Springer, Berlin, 1999.
- [4] R. HARTMANN AND P. HOUSTON, *Adaptive discontinuous Galerkin finite element methods for the compressible Euler equations*, J. Comput. Phys., 183 (2002), pp. 508–532.
- [5] K. HILLEWAERT AND N. CHEVAUGEON, *Hierarchic multigrid iteration strategy for the discontinuous Galerkin solution of the steady Euler equations*, Int. J. Numer. Methods Fluids, 6 (2002), pp. 1–20.
- [6] H. LU, *High Order Finite Element Solution of Elastohydrodynamic Lubrication Problems*, Phd thesis, School of Computing, University of Leeds, 2006.
- [7] H. LU, M. BERZINS, C. E. GOODYER AND P. K. JIMACK, *High order discontinuous Galerkin method for elastohydrodynamic lubrication line contact problems*, Common. Numer. Meth. Eng., 21 (2005), pp. 643–650.
- [8] H. LUO, J. D. BAUM AND R. LOHNER, *A  $p$ -multigrid discontinuous Galerkin method for the Euler equations on unstructure grids*, J. Comput. Phys., 211 (2006), pp. 767–783.
- [9] I. ODEN, J. T. BABUSKA AND C. E. BAUMANN, *A discontinuous hp finite element method for diffusion problems*, J. Comput. Phys., 146 (1998), pp. 495–519.
- [10] P.-O. PERSSON AND J. PERAIRE, *Sub-cell shock capturing for discontinuous Galerkin methods*, 44th AIAA Aerospace Sciences Meeting and Exhibit, Reno, Nevada, 9-12 January (2006).